A Closed-Loop Neurorobotic System for Investigating Braille-Reading Finger Kinematics

Jérémie Pinoteau[1,⋆,⋆⋆], Luca Leonardo Bologna[1,⋆], Jesús Alberto Garrido[2], and Angelo Arleo[1]

[1] Adaptive NeuroComputation Group, Unit of Neurobiology of Adaptive Processes, UMR 7102, CNRS–University Pierre and Marie Curie P6, 75005, Paris, France
{jeremie.pinoteau,luca.bologna,angelo.arleo}@upmc.fr
http://www.anc.upmc.fr

[2] Department of Cellular-Molecular Physiological and Pharmacological Sciences, University of Pavia, 27100, Pavia, Italy
jesus.garrido@unipv.it

Abstract. We present a closed-loop neurorobotic system to investigate haptic discrimination of Braille characters in a reading task. We first encode tactile stimuli into spiking activity of peripheral primary afferents, mimicking human mechanoreceptors. We then simulate a network of second-order neurones receiving the primary signals prior to their transmission to a probabilistic classifier. The latter estimates the likelihood distribution of all characters and uses it to both determine which letter is being read and modulate the reading velocity.

We show that an early discrimination of the entire Braille alphabet is possible at both first and second stages of the somatosensory ascending pathway. Furthermore, 89% of the characters are correctly recognised in a constant-velocity reading task, while a closed-loop modulation of the speed allows for faster scanning and movement kinematics similar to the ones observed in humans –though with a lower classification rate.

Keywords: Dynamic haptic discrimination, Braille reading, Spiking neural networks.

1 Introduction

Braille reading involves haptic texture perception as well as cognitive processing and motor control operations. At the peripheral afferent level, the forces exerted by Braille character dots on the fingertip induce visco-elastic deformations of the skin which stimulate the mechanoreceptors innervating the epidermis. The information conveyed by first afferent neural signals is transmitted to the spinal cord as well as to the cuneate nucleus (CN) of the brainstem. The CN projects to several areas of the central nervous system, including the cerebellum and the thalamus, which in turn transfer the information to the primary somatosensory cortex. Processing along this pathway allows haptic

⋆ J.P. and L.L.B. contributed equally to this work.
⋆⋆ Corresponding author.

P. Isokoski and J. Springare (Eds.): EuroHaptics 2012, Part I, LNCS 7282, pp. 407–418, 2012.

information to be interpreted and leads to adaptive motor responses affecting the reading finger's movement kinematics. In fact, a Braille readers' fingertip undergoes several accelerations during character scanning. These changes in velocity are common to all subjects and appear to originate mainly from motor control mechanisms. Nonetheless, cognitive (i.e. linguistic) processes are shown to also affect velocity modulation, and the role of lexical, sub-lexical and semantic processing is currently being investigated [1], [2].

Here, we propose a neurorobotic framework to study active sensing during fine haptic discrimination of Braille characters. We simulate skin indentation protocols in which Braille-like tactile stimuli are dynamically scanned by an artificial touch sensor. Deformation signals act as inputs to a network of leaky-integrate-and-fire neurones (LIF), which perform an analogue-to-spike conversion and mimick the role of cutaneous mechanoreceptors. In particular, we model the activity of Slow Adapting type I (SA-I) primary afferents, in terms of both spiking discharge and receptive fields (see [3], for a recent review). LIF neurones project onto a second order network modelling CN responses through a population of Spike Response Model (SRM) [4] units. Downstream from the CN, a naive Bayesian classifier computes the probability distribution of all Braille characters online. The likelihood distributions are ultimately used to discriminate the letter currently scanned and devise an adapted velocity trajectory optimising the scanning/discrimination time.

2 Material and Methods

Figure 1 shows the complete robotic setup. We use a set of 26 different probes, reproducing a scaled version (1:1.67) of all Braille characters, to stimulate an artificial touch sensor in order to simulate the human fingertip deformations exerted by Braille dots. The touch sensor is rubbed over the Braille alphabet and its analogue responses are encoded and decoded by the simulated first- and second-order afferents (mechanoreceptors and cuneate neurones respectively). CN output activity is finally interpreted by a probabilistic classifier to perform character discrimination and adaptive speed control.

2.1 The Artificial Touch Sensor

An artificial skin prototype[1] [6], [7] was initially used to collect and characterise a first dataset of analogue responses to Braille character indentations. This artificial fingertip consists of 24 capacitive square sensors disposed according to a rectangular grid layout. Each sensor has a dimension of approximately 3 mm and the inter-centre distance is 4 mm, for a total sensitive surface of approximately 18×23 mm (Fig. 1B). The array is covered by a 2.5 mm thick neoprene layer aiming at modulating the pressure exerted on the sensors. The response strength of each sensor is proportional to the indentation level and ranges from 0 to 189 femtoFarads (fF). The acquisition frequency of each capacitive pad is 20 Hz.

[1] Developed at the Italian Institute of Technology (IIT), Genoa, Italy.

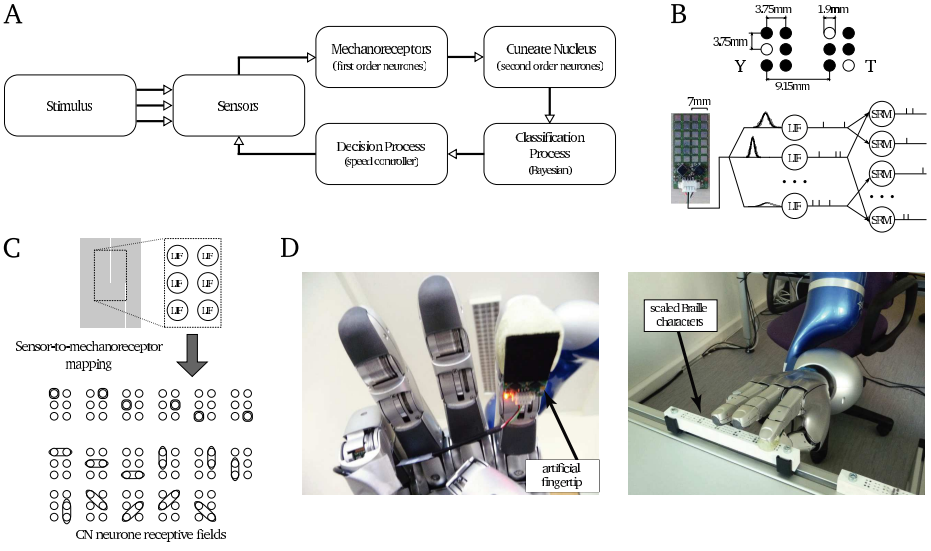

Fig. 1. *Overview of the entire encoding/decoding pathway and robotic setup*. (A) From left to right. We employ Braille characters as tactile stimuli to indent a capacitive artificial touch sensor. A network of Leaky-Integrate-and-Fire (LIF) neurones [5] converts analogue signals from the sensor into spiking activity, mimicking fingertip mechanoreceptors. LIF neurones project onto a network of Spike-Response-Model units [4] implementing second order cuneate nucleus (CN) cells. The outgoing activity is decoded by a Naive Bayesian Classifier whose output allows a speed controller to devise an optimal velocity for the fingertip movement. (B) Top: Examples of scaled Braille characters used as stimuli. Bottom: schematic representation of the encoding process, from artificial sensor signals to CN neurones output activity. (C) Top: LIF neurones modelling mechanoreceptor activity fulfil a topological mapping of fingertip regions. Bottom: CN cell receptive fields are built so as to collect the activity of either a single cell or different possible combinations of two or three adjacent mechanoreceptors. (D) The artificial fingertip mounted on a robotic hand/arm setup (Institute of Robotics and Mechatronics, German Aerospace Center ©).

We developed a simulator reproducing the responses of the artificial fingertip and offering a greater flexibility in data generation and experimental protocols [7]. We modelled the touch sensor responses by means of Gaussian kernels of amplitude 55 fF and standard deviation 1.6 mm. Additionally, we added a white noise to the amplitude and standard deviation of the signals (2.5 fF and 0.1 mm respectively) and we modelled possible position errors due to the experimental setup by adding a Gaussian noise to the location of each stimulus (sd = 0.1 mm).

2.2 Primary Afferent Coding: Analogue-to-Spike Transduction

We implement a network of 12 leaky integrate-and-fire (LIF) neurones [8], [5] to convert analogue touch sensor outputs into spike train patterns (Fig. 1C). We map the capacitance values provided by the touch sensors into current intensities $I(t)$ driving the LIF neurones by applying a multiplicative gain factor of -390 pA/fF (determined

by comparing output LIF spike trains against recorded mechanoreceptor responses [9]). The dynamics of the membrane potential $V(t)$ of each LIF neurone is:

$$C \cdot \frac{dV(t)}{dt} = -g \cdot (V(t) - V_{\text{leak}}) - I(t) \tag{1}$$

where $C = 0.5$ nF denotes the membrane capacitance, $g = 25$ nS the passive conductance, $V_{\text{leak}} = -70$ mV the resting membrane potential, and $I(t)$ the total synaptic input of a neurone. The membrane time constant is then $\tau = C/g = 20$ ms. Whenever the membrane potential $V(t)$ reaches the threshold $V_{\text{thr}} = -50$ mV the neurone emits an action potential. Then, its membrane potential is reset to $V_{\text{reset}} = -100$ mV and the dynamics of $V(t)$ is frozen during a refractory period $\Delta t_{\text{ref}} = 2$ ms. We also use a "threshold fatigue" [5] to model the phenomenon of "habituation". It consists in increasing the threshold V_{thr} by a value A_{thr} each time the neurone discharges, making it harder for the neurone to spike again (i.e. preventing it from responding in a highly tonic manner even in the presence of strong inputs). In the absence of spikes, the threshold decreases exponentially back to its resting value V_{restThr}:

$$\frac{dV_{\text{thr}}(t)}{dt} = -\frac{V_{\text{thr}}(t) - V_{\text{restThr}}}{\tau_{\text{thr}}} \tag{2}$$

with $\tau_{\text{thr}} = 100$ ms, $V_{\text{restThr}} = -50$ mV and $A_{\text{thr}} = 50$ mV.

2.3 Second-Order Processing in the Cuneate Network

We model individual cuneate cell responses by means of 49 SRM neurones [4] (see [10], for a previous use of the model) implemented through a simulation environment [11] optimised to reduce execution time. We include a noise model (i.e. escape noise) that follows a stochastic process, thereby providing a linear probabilistic neuronal model.

An input spike arrival at time t induces a membrane potential depolarisation under the form of an EPSP (excitatory postsynaptic potential) $\Delta V(t)$ described by:

$$\Delta V(t) \propto \sqrt{t} \exp(-t/\tau) \tag{3}$$

where the parameter $\tau = 2$ ms determines the decay time constant of the EPSP. If several spikes excite the neurone within a short time window, the EPSPs add up linearly:

$$V(t) = V_{\text{r}} + \sum_{i,j} w_{\text{i}} \, \Delta V(t - \hat{t}_{\text{i}}^{\text{j}}) \tag{4}$$

where i denotes presynaptic neurones, j indexes the spikes emitted by a presynaptic neurone i at times $\hat{t}_{\text{i}}^{\text{j}}$, and $V_{\text{r}} = -70$ mV is the resting potential. The term w_{i} indicates the synaptic weight of the projection from the presynaptic unit i, defined as:

$$w_{\text{i}} = W \cdot w_{\text{i}}^{0,1} \tag{5}$$

with factor W determining the upper bound of the synaptic efficacy, and $w_{\text{i}}^{0,1}$ being constrained within the range $[0, 1]$. We use $W = 0.04$ in our simulations. At each time step, a function $g(t)$ is defined as:

$$g(t) = r_0 \log\left(1 + \exp\left(\frac{V(t) - V_0}{V_{\text{f}}}\right)\right) \tag{6}$$

where the constants $r_0 = 11$ Hz, $V_0 = -65$ mV, $V_f = 0.1$ mV are the instantaneous firing rate, the probabilistic threshold potential, and a gain factor, respectively. A function $A(t)$ determines the refractoriness property of the neurone:

$$A(t) = \frac{(t - \hat{t} - \tau_{abs})^2}{\tau_{rel}^2 + (t - \hat{t} - \tau_{abs})^2} \mathscr{H}(t - \hat{t} - \tau_{abs}) \tag{7}$$

where $\tau_{abs} = 3$ ms and $\tau_{rel} = 9$ ms denote the absolute and relative refractory periods, respectively, $\hat{t}$ the time of the last spike emitted, and $\mathscr{H}$ the Heaviside function. Finally, the functions $g(t)$ and $A(t)$ allow the probability of firing $p(t)$ to be computed:

$$p(t) = 1 - \exp\Big(-g(t)A(t)\Big) \tag{8}$$

We implement the synaptic connections between mechanoreceptors and cuneate nucleus neurones so as to generate the receptive fields shown in Fig. 1C. Each CN neurone receives non-plastic inputs from either one or a group of two/three adjacent mechanoreceptors depending on the stimulus (see Fig. 1 for details). The dimension and shape of the receptive fields and the synaptic weight distribution of the mechanoreceptor-to-CN projections allow topographical information to be maintained at the level of the second order output space. Also, thanks to the adopted connectivity layout, CN neurones collecting signals from large receptive fields mirror both single primary neurone activation and multiple co-activations, thus enriching the population's spiking dynamics.

2.4 Assessing Neurotransmission Reliability: Metrical Information Analysis

In order to decode neural activities and quantify fine touch discrimination, we apply the recently defined metrical mutual information $I^*(R;S)$ [12]. Unlike Shannon's definition of mutual information [13],[14], this measure takes into account the metrical properties of the spike train space [15],[16],[17] and has been proven to be suitable to decode the responses of human mechanoreceptors obtained via microneurography recordings [10],[12]. The definition of $I^*(R;S)$ relies on a similarity function based on the distances between spike train responses elicited by the entire set of stimuli. The Victor and Purpura Distance was used in the definition of the metrical information [15]. This specific spike metric makes it possible to modulate the importance given to temporal (and rate) coding in the mapping of the spike train space through a cost parameter.

The perfect discrimination condition corresponds to maximum $I^*(R;S)$ and zero conditional entropy $H^*(R|S)$ [12]. It occurs when the size of the largest cluster of responses (to the same stimulus) becomes smaller than the smallest distance between all clusters of responses [12].

2.5 Online Classification of Braille Characters: Naive Bayesian Classifier

To discriminate Braille characters during the reading task, we trained a Naive Bayesian Classifier (NBC) via multinomial distributions. This learning algorithm belongs to the family of probabilistic classifiers relying on Bayes' rule to compute the posterior probability of the sample classes. Despite its simplicity, the NBC has proven to be fast and

efficient even when the feature independence hypothesis underlying its application is not fulfilled [18],[19].

Braille characters (i.e. dataset classes) are defined from the spike train activity encoded after the touch sensor signals. With the aim of performing a fast classification, we built the training dataset in two steps. We first swiped the fingertip over the complete set of 26 Braille characters and collected the cuneate neurones' responses. We then binned the 49 CN cells spiking activity with temporal windows of increasing length (see Fig. 3A). The bin size increment was fixed at 10 ms. Each temporal bin is characterised by the spatiotemporal organisation of the firing activity it encloses and is labelled with the corresponding character. The properties of the spiking activity present in each bin (e.g. spike times, spiking neurones), contribute to building a model associating specific Braille characters to the different patterns of activity. In the online task, a character detection occurs whenever the probability distribution's peak exceeds the 90% threshold.

2.6 From Classification to Reading Velocity Control: Kurtosis-Based Assessment of the Likelihood Distribution

Given the procedure adopted to build the activity dataset and the small time bin chosen as temporal increment, characters' probability distributions can be measured frequently while reading. We use such information to compute the excess Kurtosis index which indicates the extent to which a probability distribution is peaked around its values.

At each simulation time step, the Kurtosis index gradient is used to adapt the reading velocity. A positive value indicates that the distribution is narrowing. Such a convergence reflects a decrease in the uncertainty on the character being scanned and triggers a velocity increase proportional to the gradient value. Differently, a distribution's widening induces a deceleration. We investigate whether this velocity modulation decreases the classification time as compared to a constant velocity movement.

3 Results

3.1 Characterisation of Mechanoreceptor Responses

In a previous study, we compared simulated and human mechanoreceptors responses to fingertip skin indentations through Braille-character probes [20]. Modelled primary afferents exhibit receptive fields qualitatively similar to those of human Slow Adaptive I (SA-I) mechanoreceptors, in terms of shape, dimensions and signal-to-noise ratio (see Fig. 2A). SA-I primary afferents show a topological mapping (i.e. their activity correlates with the area of stimulation), demonstrating their role in encoding spatial discontinuities [3]. Fast Adaptive I (FA-I) mechanoreceptors have similar spatial properties but, thus far, no clear experimental evidence has shown whether SA-I or FA-I afferents primarily carry the information needed for Braille character recognition [21].

The first spike jitter distributions of simulated and human SA-I mechanoreceptors, are statistically equivalent in terms of median and shape (Mann-Whitney U test, $P > 0.11$; Kolmogorov-Smirnov test, $P > 0.076$), despite a time lag in the simulated responses of about 2 ms (see Fig. 2B). Thus, modelled mechanoreceptors present the same variability in spike latencies as SA-I afferents, but on a larger time scale.

3.2 Information Content of First and Second Order Tactile Afferent Responses

We investigate neurotransmission reliability at both the first and second order neurones level by decoding mechanoreceptor and CN cell responses to the entire Braille alphabet during scanning. More specifically, we focus on the evolution of the information content over time with the aim of quantifying how rapidly a perfect discrimination of all characters can be achieved after the stimulus onset.

Figure 2C (Top) illustrates the evolution of the metrical information and conditional entropy as spikes flow in while scanning the entire Braille stimuli set at a constant velocity of 30 mm/s. The cost in the Victor and Purpura Distance was chosen so to allow the earliest possible perfect discrimination.

At the mechanoreceptor level, first spikes occur at around 100 ms, and 250 ms later the condition for an errorless stimulus reconstruction is satisfied. In comparison, a small delay is observed at the CN output level, and almost perfect discrimination is possible just as soon. As expected, the metrical information curve exhibits a plateau starting at around 200 ms and lasting approximately 75 ms. This corresponds to the stimulation phase during which the fingertip is already in contact with the first column of Braille dots while the second does not stimulate any sensor yet. The information value at the plateau is about half of the total amount of information transmitted.

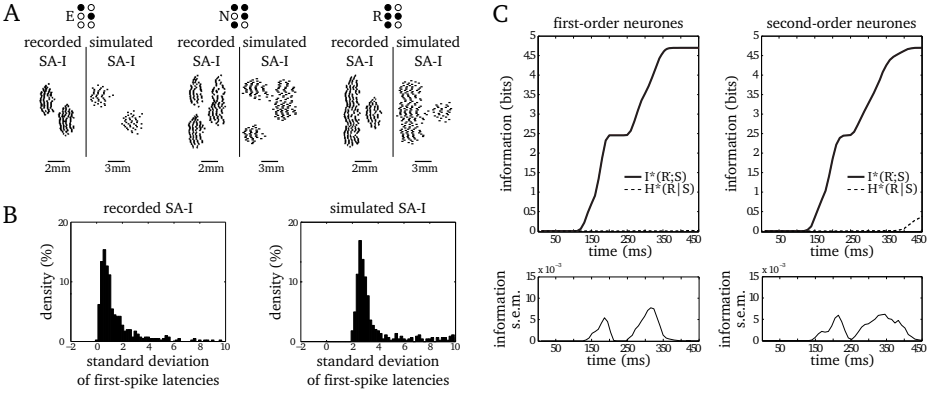

Fig. 2. *Characterisation of mechanoreceptor properties and theoretical information analysis of first and second order afferent responses to Braille stimuli*. (A) Spatial event plots of human SA-I mechanoreceptor responses to scanned Braille characters 'e', 'n' and 'r' and their simulated counterparts (recorded sections adapted from [21]). (B) Distribution of standard deviations (SD) of first-spike latencies for both SA-I (left) and simulated (right) mechanoreceptor responses. (C) Top: Time course of metrical information (full line) and conditional entropy (dashed line) at the output of LIF (left) and CN (right) neurones, as the fingertip scans the Braille characters at 30 mm/s. The 26 Braille characters serve as stimuli, with 20 repetitions per stimulus used. First spikes occur at around 100 ms, and the perfect discrimination condition is reached about 250 ms later. Bottom: Information variability, measured as mean standard error, over time.

3.3 Classification of Braille Characters in a Reading Task

We collect a dataset of character samples and fit a probabilistic classifier to estimate the posterior probability of Braille characters while reading. When the NBC fitting parameters are used for offline classification, a near perfect discrimination is possible as soon as enough spikes are processed by the classifier. In fact, as a result of the binning procedure adopted, data samples built by gathering the spiking activity in small temporal windows (cf. Sect. 2.5) do not carry enough information to allow a correct discrimination; on the contrary, considering longer periods leads to a decrease in the uncertainty (see Fig. 3B). A clear example of the evolution of probability distributions over time is given in Fig. 3C. At the beginning of the scanning movement, the spiking activity of CN neurones responding to letter 'r' (Fig. 3C, left panel) does not allow to distinguish between 'r' and the other Braille characters with a similar dot disposition (i.e. 'l', 'p', 'q', 'v' - see Fig. 1C, left panel inset). But, as time evolves, probability distributions start to peak indicating that the uncertainty decreases till a correct classification is possible (maximal probability reached for letter 'r'). A similar example is shown for letter 'e' (see Fig. 3C, right panel).

In online simulations, when the classifier is tested with a constant scanning velocity of 30 mm/s, 89% of the scanned characters are correctly discriminated (10% false positive, 1% no classification). Differently, if a speed modulation is adopted, the NBC's performance decreases to 78% of correct classifications (18% of false positives, 4% no classification). However, the discrimination of most letters is sensibly the same in both cases. The observed loss in overall performance is mostly due to couples of letters (e.g. 'a' and 'c') whose recognition rate fall considerably (down to approximately 45%) given to the similarity between character dot patterns.

3.4 Online Reading Velocity Modulation

The methodology we adopted for building the spiking-activity based dataset, lends itself to a frequent computation of Braille character probability distributions. We asked whether the probabilities evolution over time could be seen as a possible mechanism underlying the changes in reading speed of blind readers that can be attributed to lexical and sub-lexical processes. Thus, we computed the Kurtosis index gradient on probability distributions at each time step (cf. Sect. 2.6) and, upon multiplication by a constant factor, used it to modulate the reading speed (see Fig. 4A).

Following the velocity modulation approach, global reading performances improve. At the end of the scanning of a single character, the average velocity adopted through modulation is higher than the finger's initial velocity (i.e. when it first encounters the character) which would have been maintained in the absence of dynamic changes to the reading speed (i.e. constant velocity scanning). For a base velocity of 30 mm/s, the speed modulation allowed the average scanning velocity to increase to 35.4 mm/s. Moreover, we observed an average number of 8.6 accelerations per character (see Fig. 4B). This result is coherent with what was observed in human Braille reading experiments where the influence of lexical (i.e. words) and sub-lexical (i.e. characters) content on fingertip velocity intermittencies are investigated [2].

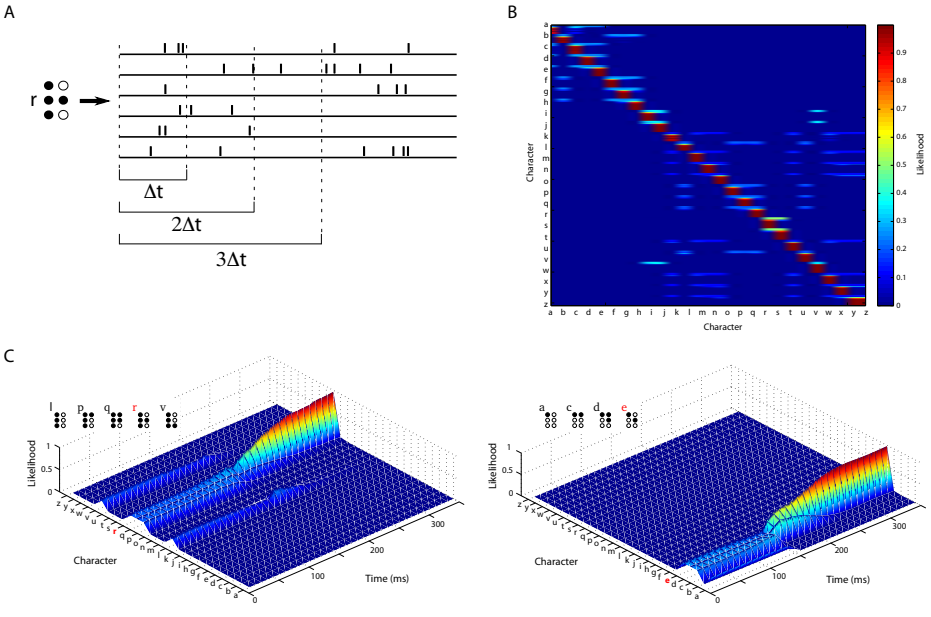

Fig. 3. *Binning procedure and Naive Bayesian classifier output likelihood distributions*. (A) CN spiking activity is binned following time windows of increasing size ($n \times \Delta t$). (B) Confusion matrix of training samples (100 samples per character), indicating classification probabilities as determined by the Bayesian classifier. For each character, samples of increasing duration are considered (matrix rows). Small bins capture little activity and the classifier is not able to distinguish between different patterns (light blue values). Differently, larger bins collect enough information to allow character discrimination (red values). (C) Expanded sections of panel B for letters 'r' (left) and 'e' (right). Initially, characters with similar dot patterns (reported in the insets) are equally probable. As time increases, more activity is collected and the probability distribution peaks on a single value (indicating the character being read).

4 Discussion

Dynamic haptic discrimination in humans involves several processes at different levels of abstraction (e.g. encoding/decoding of afferent signals, sensorimotor control, decision making). At the periphery of the somatosensory pathway, primary afferents precisely encode tactile signals and reliably convey them to downstream structures [9]. At the same time, tactile information is used by cognitive and motor processes to interpret the stimulus and adapt limbic movements to optimise texture exploration.

In Braille reading, the perceptual, cognitive and motor aspects reciprocally and dynamically interact. Notably, it has been demonstrated that blind subjects continuously change reading velocity while surfing a dotted character line, regardless of the semantic of the patterns they encounter and often unconsciously [1]. Nonetheless, besides motor related velocity intermittencies, word frequency and sub-lexical content contribute to the pervasive changes of the reading speed [2].

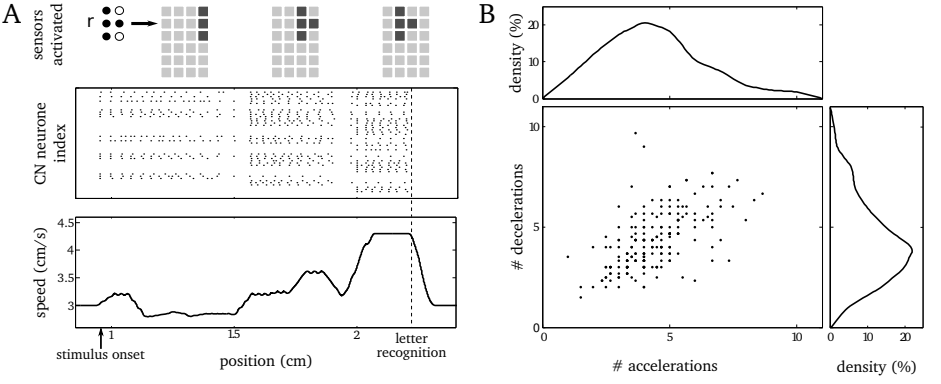

Fig. 4. *CN activity modulation and dynamic adaptation of the reading speed*. (A) Top (left to right): Sensor activation as the stimulus is scanned. Center: The activity of CN neurones is shown as a function of the stimulus position relative to the fingertip. Bottom: Modulation of the reading speed along the Braille line. The fingertip initially moves at a constant velocity. As the character enters the sensor area, the scanning speed starts being modulated on the basis of the computed character probability distributions. Soon after the stimulus has been entirely covered by the finger, a sudden increase in velocity is observed, indicating a peak in the probability distribution. After the classification is performed, the velocity is reset to a constant value (i.e. 30 mm/s). (B) Scatter plot: Number of accelerations and decelerations observed during individual character scanning, for a representative set of samples. Each dot corresponds to a mean value computed over 3 trials of a single character. Depending on the complexity of the pattern being read, a variable number of velocity changes is required. Top and Bottom right: Number of accelerations and decelerations probability distributions.

In this study, we propose a neuro-inspired closed-loop system to investigate haptic discrimination during Braille reading. We integrate tactile information coding at the neuronal level with a probabilistic framework for dynamic stimulus classification and adaptive motor control. We convert the analogue signals from an artificial fingertip into spiking activity and we apply an information theoretical analysis to the first and second afferent output stages. We finally interpret online the output of the second order Cuneate Nucleus neurones through a Naive Bayesian Classifier and use the character probability distribution to determine an efficient reading velocity.

Our results show that signals at the earliest stages of the haptic ascending pathway are conveyed as to allow a complete and fast discrimination by downstream decoders. We demonstrate that a probabilistic approach allows to efficiently recognise all Braille characters in an online reading task and we show that a dynamic adaptation of the finger velocity allows a faster recognition. Finally, we observe a number of accelerations which is coherent with human experiments outcomes and we argue that a probabilistic signal interpretation can account for the velocity intermittencies not induced by motor control operations.

We are currently investigating how the interferences created by different scanning velocities on the activity of CN neurones influence the classification process. We are also integrating a cerebellar model in the closed-loop system to explore in further detail motor and cognitive contributions to velocity corrections. We finally propose to

investigate whether the speed modulation can help improve discrimination performance in the case of noisy fingertip movements.

Acknowledgments. Granted by the EC Project SENSOPAC (no. IST-028056-IP) and by the Délégation Générale de l'Armement (DGA). The authors thank the CASPUR Consortium (www.caspur.it) for providing the high performance computing facilities.

References

1. Hughes, B., Van Gemmert, A.W.A., Stelmach, G.E.: Linguistic and perceptual-motor contributions to the kinematic properties of the braille reading finger. Human Movement Science 30(4), 711–730 (2011)
2. Hughes, B.: Movement kinematics of the braille-reading finger. Journal of Visual Impairment & Blindness 105(6), 370–381 (2011)
3. Johansson, R.S., Flanagan, J.R.: Coding and use of tactile signals from the fingertips in object manipulation tasks. Nature Reviews Neuroscience 10(5), 345–359 (2009)
4. Gerstner, W., Kistler, W.: Spiking Neuron Models. Cambridge University Press (2002)
5. Chacron, M.J., Pakdaman, K., Longtin, A.: Interspike interval correlations, memory, adaptation, and refractoriness in a leaky integrate-and-fire model with threshold fatigue. Neural Computation 15(2), 253–278 (2003)
6. Cannata, G., Maggiali, M., Metta, G., Sandini, G.: An embedded artificial skin for humanoid robots. In: Proc. IEEE International Conference on Multisensor Fusion and Integration for Intelligent Systems MFI 2008, pp. 434–438 (2008)
7. Bologna, L.L., Brasselet, R., Maggiali, M., Arleo, A.: Neuromimetic encoding/decoding of spatiotemporal spiking signals from an artificial touch sensor. In: Proceedings of the 2010 International Joint Conference on Neural Networks (IJCNN), vol. 10, pp. 1–6 (2010)
8. Lapicque, L.: Recherches quantitatives sur l'excitation électrique des nerfs traitée comme une polarisation. Journal de Physiologie et Pathologie General 9, 620–635 (1907)
9. Johansson, R.S., Birznieks, I.: First spikes in ensembles of human tactile afferents code complex spatial fingertip events. Nature Neuroscience 7(2), 170–177 (2004)
10. Brasselet, R., Johansson, R., Arleo, A., Bengio, Y., Schuurmans, D., Lafferty, J., Williams, C., Culotta, A.: Optimal context separation of spiking haptic signals by second-order somatosensory neurons. In: Advances in Neural Information Processing Systems 22, pp. 180–188 (2009)
11. Carrillo, R.R., Ros, E., Boucheny, C., Coenen, O.J.D.: A real-time spiking cerebellum model for learning robot control. BioSystems 94(1-2), 18–27 (2008)
12. Brasselet, R., Johansson, R.S., Arleo, A.: Quantifying neurotransmission reliability through metrics-based information analysis. Neural Computation 23(4), 852–881 (2011)
13. Shannon, E.: A mathematical theory of communication. The Bell System Technical Journal 27, 379–423, 623–656 (1948)
14. Rieke, F., Warland, D., de Ruyter van Stevenick, R., Bialek, W. (eds.): Spikes: Exploring the neural code. MIT Press, Cambridge (1997)
15. Victor, J.D., Purpura, K.P.: Nature and precision of temporal coding in visual cortex: a metric-space analysis. Journal of Neurophysiology 76(2), 1310–1326 (1996)
16. Schreiber, S., Fellous, J.M., Whitmer, D., Tiesinga, P., Sejnowski, T.J.: A new correlation-based measure of spike timing reliability. Neurocomputing 52-54, 925–931 (2003)
17. van Rossum, M.C.: A novel spike distance. Neural Computation 13(4), 751–763 (2001)
18. Zhang, H.: The optimality of naive Bayes. In: Proceedings of the FLAIRS Conference, vol. 1(2), pp. 3–9. AAAI Press (2004)

19. Truccolo, W., Friehs, G.M., Donoghue, J.P., Hochberg, L.R.: Primary motor cortex tuning to intended movement kinematics in humans with tetraplegia. The Journal of Neuroscience 28(5), 1163–1178 (2008)
20. Bologna, L.L., Pinoteau, J., Brasselet, R., Maggiali, M., Arleo, A.: Encoding/decoding of first and second order tactile afferents in a neurorobotic application. Journal of Physiology-Paris 105(1-3), 25–35 (2011)
21. Phillips, J., Johansson, R., Johnson, K.: Representation of braille characters in human nerve fibres. Experimental Brain Research 81(3), 589–592 (1990)